



## Article

# Phenomenological Equation of State of Strongly Interacting Matter with First-Order Phase Transitions and Critical Points

Stefan Typel <sup>1,2\*</sup> and David Blaschke <sup>3,4,5</sup>

<sup>1</sup> Institut für Kernphysik, Technische Universität Darmstadt, Schlossgartenstraße 9, 64289 Darmstadt, Germany; stypel@ikp.tu-darmstadt.de

<sup>2</sup> GSI Helmholtzzentrum für Schwerionenforschung GmbH, Planckstraße 1, 64291 Darmstadt, Germany; s.typel@gsi.de

<sup>3</sup> Institute of Theoretical Physics, University of Wrocław, Pl. M. Borna 9, 50-204 Wrocław, Poland; david.blaschke@gmail.com

<sup>4</sup> Bogoliubov Laboratory for Theoretical Physics, Joint Institute of Nuclear Research, 141980 Dubna, Russia

<sup>5</sup> National Research Nuclear University (MEPhI), Kashirskoe shosse 31, 115409 Moscow, Russia

\* Correspondence: s.typel@gsi.de; Tel.: +49-6159-71-2744

Academic Editor: name

Received: date; Accepted: date; Published: date

**Abstract:** An extension of the relativistic density functional approach to the equation of state for strongly interacting matter is suggested that generalizes a recently developed modified excluded-volume mechanism to the case of temperature- and density-dependent available-volume fractions. A parametrization of this dependence is presented for which, at low temperatures and suprasaturation densities, a first-order phase transition is obtained. It changes for increasing temperatures to a crossover transition via a critical endpoint. This provides a benchmark case for studies of the role of such a point in hydrodynamic simulations of ultrarelativistic heavy-ion collisions. The approach is thermodynamically consistent and extendable to finite isospin asymmetries that are relevant for simulations of neutron stars, their mergers, and core-collapse supernova explosions.

**Keywords:** Equation of state; QCD matter; phase transition; critical point; modified excluded-volume mechanism

## 1. Introduction

The simulation of astrophysical phenomena, such as core-collapse supernovae (CCSN) or neutron-star (NS) mergers, requires a careful modeling of strongly interacting matter in a wide range of densities and temperatures. The same applies to the theoretical description of heavy-ion collisions (HIC) that study compressed baryonic matter in the laboratory from low to high beam energies. The properties of such matter are represented by the equation of state (EoS) that provides information on pressure, entropy, energies, and other thermodynamic variables of interest.

A particular feature of QCD matter is the supposed phase transition (PT) from hadronic matter to quark matter when density or temperature increase to sufficiently high values. A strong first-order PT could allow for the existence of a third branch of compact stars and the occurrence of the twin-star phenomenon [1–3]. Signals of the PT might also have direct consequences in dynamical processes when matter in the quark phase expands and cools down, e.g., the release of a second neutrino burst in CCSN [4–6]. For a recent review on the role of the EoS in CCSN simulations, see [7].

The theoretical description of the hadron–quark PT in strongly interacting matter often relies on a construction employing different models for the two phases. With such an approach, the coexistence

line of the first-order PT will usually connect a point on the zero-temperature axis at finite baryon chemical potential  $\mu_B$  with a point at finite temperature  $T$  on the zero baryon chemical potential axis. By this construction, the QCD hadron–quark PT is of first order in the whole temperature–density plane, see for instance [8]. However, from lattice QCD studies, it is known that there is a smooth crossover at  $\mu_B = 0$  with increasing  $T$  [9,10], so at least one critical point at finite  $\mu_B$  and  $T$  is expected to exist. Other possibilities are that the character of the transition is crossover all over the QCD phase diagram [11] or, as is advocated in studies of the BEC-BCS crossover transition in low-temperature QCD, that a second critical endpoint exists [12–14]. Since lattice QCD studies are presently incapable of exploring the EoS close to the presumed critical point with much confidence, unified models are needed that can account for the existence of these features, see, e.g., [15]. There are dedicated microscopic models available that incorporate the major expected features in the QCD phase diagram, e.g., chiral mean-field models [16] or parity-doublet quark–hadron models [17]. Simulations of CCsN or HIC that are based on a hydrodynamic description of matter during dynamical evolution use the thermodynamic properties of matter encoded in the EoS as an input. Such data can be provided by phenomenological models that do not need to incorporate all of the details of the underlying physics.

In this work, a novel approach is introduced to provide a phenomenological EoS of baryonic matter that exhibits a first-order PT and a critical point at densities and temperatures expected in QCD matter. The parameters of the model can be adjusted to place the coexistence line at arbitrary positions in the phase diagram. The description uses an extension of a relativistic energy density functional for hadronic matter assuming a medium-dependent change in the number of degrees of freedom. This approach employs a recently developed version of a modified excluded-volume (EV) mechanism that gives a thermodynamically consistent EoS with nuclear matter properties that are consistent with present constraints. Here, we concentrate on the hadron–quark transition but not on the liquid–gas PT, which is also contained in our model. The model allows us to study the PT for arbitrary isospin asymmetries; however, only isospin-symmetric matter is considered in this first exploratory study for simplicity. In the present work, no attempt was made to reproduce the EoS of QCD matter at vanishing baryon chemical potential obtained in lattice QCD studies. With appropriately chosen EV parameters, the crossover transition with increasing temperature can be well modeled, even for imaginary chemical potentials, e.g., in a hadron resonance gas model [18]. With improved parametrizations, the structure of the phase diagram in the full space of variables, i.e., temperature, baryon density/chemical potential, and isospin asymmetry, can be investigated in the future.

The theoretical formalism of the model is presented in Section 2, which includes the main equations that define the relevant thermodynamic quantities in Section 2.1. In Section 2.2, details of the parametrization of the interaction and of the effective degeneracy factors are given. They account for the change in the number of degrees of freedom with density and temperature. The phase transitions are explored in Section 3 for isospin-symmetric matter. Conclusions follow in Section 4.

## 2. Theoretical Model

The theoretical description of strongly interacting matter in the present work is adapted from the model introduced in [19]. It combines a relativistic mean-field (RMF) approach for hadronic matter with density-dependent nucleon–meson couplings and a modified EV mechanism. Here, it is sufficient to provide only the main equations without a detailed derivation. The essential quantities that determine the position of the PT and the critical point in the phase diagram are the effective degeneracy factors that depend on the number densities of the particles and the temperature.

### 2.1. Relativistic Energy Density Functional with Modified Excluded-Volume Mechanism

The present model assumes neutrons and protons as well as their antiparticles as the basic degrees of freedom. These particles interact by the exchange of mesons, and the model effectively describes the short-range repulsion ( $\omega$  meson), the intermediate-range attraction ( $\sigma$  meson), and the

isospin dependence of the nuclear interaction ( $\rho$  and  $\delta$  mesons), as is common of RMF models. The contribution of leptons or other degrees of freedom like nuclei, hyperons or photons, as required for multi-purpose EoS for astrophysical applications [20], is not considered here.

The nucleons  $i = n, p, \bar{n}, \bar{p}$  with rest masses  $m_i$  are treated as quasi-particles of energy,

$$E_i(k) = \sqrt{k^2 + (m_i - S_i)^2} + V_i \quad (1)$$

which depends on the particle momentum  $k$  and the scalar ( $S_i$ ) and vector ( $V_i$ ) potentials. Denoting the particle chemical potentials with  $\mu_i$ , the contribution of the quasi-particles to the total pressure

$$p = \sum_i p_i + p_{\text{meson}} - p^{(r)} \quad (2)$$

of the system can be written as

$$p_i = T g_i^{(\text{eff})} \int \frac{d^3k}{(2\pi)^3} \ln \left[ 1 + \exp \left( -\frac{E_i(k) - \mu_i}{T} \right) \right] \quad (3)$$

where the medium-dependent effective degeneracy factors

$$g_i^{(\text{eff})} = g_i \Phi_i \quad (4)$$

are a product of the usual degeneracy factor  $g_i = 2$  for nucleons and the available-volume fraction  $\Phi_i$ , which is defined in Section 2.2.

The meson contribution

$$p_{\text{meson}} = \frac{1}{2} \left( C_\omega n_\omega^2 + C_\rho n_\rho^2 - C_\sigma n_\sigma^2 - C_\delta n_\delta^2 \right) \quad (5)$$

to the total pressure in Equation (2) contains the coupling factors of the mesons

$$C_j = \frac{\Gamma_j^2}{m_j^2} \quad (6)$$

given as a ratio of the density-dependent coupling functions  $\Gamma_j$  and the meson masses  $m_j$ . The source densities

$$n_j = \sum_i g_{ij} n_i^{(v)} \quad (7)$$

for vector mesons ( $j = \omega, \rho$ ) and

$$n_j = \sum_i g_{ij} n_i^{(s)} \quad (8)$$

for scalar mesons ( $j = \sigma, \delta$ ) in Equation (5) are obtained from the quasi-particle vector densities

$$n_i^{(v)} = g_i^{(\text{eff})} \int \frac{d^3k}{(2\pi)^3} f_i(k) \quad (9)$$

and scalar densities

$$n_i^{(s)} = g_i^{(\text{eff})} \int \frac{d^3k}{(2\pi)^3} f_i(k) \frac{m_i - S_i}{\sqrt{k^2 + (m_i - S_i)^2}} \quad (10)$$

with the Fermi-Dirac distribution function

$$f_i(k) = \left[ \exp \left( \frac{E_i(k) - \mu_i}{T} \right) + 1 \right]^{-1}. \quad (11)$$

The scaling factors

$$g_{n\omega} = g_{p\omega} = -g_{\bar{n}\omega} = -g_{\bar{p}\omega} = 1 \quad (12)$$

$$g_{n\rho} = -g_{p\rho} = -g_{\bar{n}\rho} = g_{\bar{p}\rho} = 1 \quad (13)$$

$$g_{n\sigma} = g_{p\sigma} = g_{\bar{n}\sigma} = g_{\bar{p}\sigma} = 1 \quad (14)$$

$$g_{n\delta} = -g_{p\delta} = g_{\bar{n}\delta} = -g_{\bar{p}\delta} = 1 \quad (15)$$

in Equations (7) and (8) determine the coupling between mesons and nucleons. They also appear in the vector potential

$$V_i = C_\omega g_{i\omega} n_\omega + C_\rho g_{i\rho} n_\rho + B_i V_{\text{meson}}^{(r)} + V_i^{(r)} \quad (16)$$

and the scalar potential

$$S_i = C_\sigma g_{i\sigma} n_\sigma + C_\delta g_{i\delta} n_\delta + S_i^{(r)} \quad (17)$$

in the quasi-particle energy (Equation (1)). The rearrangement potential

$$V_{\text{meson}}^{(r)} = \frac{1}{2} (C'_\omega n_\omega^2 + C'_\rho n_\rho^2 - C'_\sigma n_\sigma^2 - C'_\delta n_\delta^2) \quad (18)$$

contributes to the vector potential (Equation (16)) because the couplings  $\Gamma_j$  in Equation (6) are assumed to depend on the baryon density  $n_B = \sum_i B_i n_i^{(v)}$ , where  $B_i = g_{i\omega}$  is the baryon number of particle  $i$ , and the quantities  $C'_j = dC_j/dn_B$  are the derivatives of the coupling factors.

The dependence of the available-volume fractions  $\Phi_i$  in the effective degeneracy factor (Equation (4)) on the vector or scalar quasi-particle densities (9) and (10) also generates rearrangement contributions

$$V_i^{(r)} = - \sum_j p_j \frac{\partial \ln \Phi_j}{\partial n_i^{(v)}} \quad (19)$$

and

$$S_i^{(r)} = \sum_j p_j \frac{\partial \ln \Phi_j}{\partial n_i^{(s)}} \quad (20)$$

in the potentials (Equations (16) and (17)), respectively. Furthermore, there is a rearrangement term

$$p^{(r)} = p_{\text{meson}}^{(r)} + p_\Phi^{(r)} \quad (21)$$

in the total pressure (Equation (2)) with two contributions from the density dependence of the couplings

$$p_{\text{meson}}^{(r)} = -V_{\text{meson}}^{(r)} n_B \quad (22)$$

and

$$p_\Phi^{(r)} = \sum_i (n_i^{(s)} S_i^{(r)} - n_i^{(v)} V_i^{(r)}) \quad (23)$$

from the EV effects.

The free energy density of the system

$$f = \sum_i \mu_i n_i^{(v)} - p \quad (24)$$

is obtained with the total pressure (Equation (2)) and the chemical potentials of the particles  $\mu_i$ . They are not independent since, for nucleons with baryon number  $B_i$  and charge number  $Q_i$ , they are given by

$$\mu_i = B_i \mu_B + Q_i \mu_Q \quad (25)$$

with the baryon chemical potential  $\mu_B$  and the charge chemical potential  $\mu_Q$ . Only the latter two are independent quantities. For the internal energy density

$$\varepsilon = f + Ts \quad (26)$$

the entropy density

$$s = - \sum_i g_i^{(\text{eff})} \int \frac{d^3k}{(2\pi)^3} [f_i \ln f_i + (1 - f_i) \ln (1 - f_i)] + \sum_i p_i \frac{\partial \ln \Phi_i}{\partial T} \quad (27)$$

is needed. Besides the standard contribution depending on the distribution functions  $f_i$ , there is a term from the possible temperature dependence of the available-volume fractions  $\Phi_i$ . In order to guarantee the third law of thermodynamics, i.e.,  $\lim_{T \rightarrow 0} s = 0$ , the temperature derivative of the available-volume fractions has to vanish for  $T \rightarrow 0$ . After solving the equations above for a given  $T$ ,  $\mu_B$ , and  $\mu_Q$ , a fully consistent thermodynamic EoS is obtained. For practical purposes, however, the baryon density  $n_B$  and the hadronic charge fraction

$$Y_q = \frac{\sum_i Q_i n_i^{(v)}}{n_B} \quad (28)$$

are used as independent variables instead of  $\mu_B$  and  $\mu_Q$ .

A possible shortcoming of models that consider EV effects is the potential appearance of a superluminal speed of sound in certain regions of the space of thermodynamic variables, see, e.g., [21,22]. This causality constraint has to be checked case by case depending on the specific implementation of the EV mechanism.

## 2.2. Available-Volume Fractions and Model Parameters

For a quantitative evaluation of the EoS in the present approach, the functional forms of the meson–nucleon couplings  $\Gamma_j$  and the available-volume fractions  $\Phi_i$  have to be specified as well as all parameters. Here, we use the masses of nucleons and mesons and the coupling functions of the DD2 parametrization presented in [23]. It only considers  $\omega$ ,  $\rho$ , and  $\sigma$  mesons for the effective description of the nuclear interaction but not the  $\delta$  mesons. The parameters were obtained by fitting observables (binding energies, radii, etc.) of selected nuclei. With this set, the EoS of nuclear matter at zero temperature exhibits characteristic nuclear matter parameters, e.g., the saturation density ( $n_{\text{sat}} = 0.149065 \text{ fm}^{-3}$ ), binding energy at saturation ( $B = 16.02 \text{ MeV}$ ), incompressibility ( $K = 242.7 \text{ MeV}$ ), symmetry energy ( $J = 32.73 \text{ MeV}$ ), and slope ( $L = 57.94 \text{ MeV}$ ), that are consistent with modern constraints from experiment and theory.

EV effects are frequently employed to describe an effective repulsive interaction between particles, in particular in calculations of the EoS in the framework of hadron resonance gas models, see, e.g., [24]. For zero baryon density, a comparison of the resulting EoS with results from lattice QCD calculations can be used to fix the volume parameters. If a finite volume  $v_i$  is attributed to each particle  $i$ , the available volume for the motion of the particle is reduced from the total system volume  $V$  to  $V\Phi^{(cl)}$  with the classical available-volume fraction

$$\Phi^{(cl)} = 1 - \sum_i v_i n_i^{(v)}. \quad (29)$$

Clearly, there is a limiting density above which a compression of the system becomes impossible. In general, the volumes and available-volume fractions can depend on the particle species, and the EV mechanism can be used to suppress particles, e.g., nuclei, in a mixture, causing them to disappear above a certain density, see, e.g., [25] for applications to the low-temperature and low-density EoS in astrophysical simulations.

In [19], the interpretation of the EV mechanism was changed by moving the factor  $\Phi_i$  from the system volume  $V$  to the degeneracy factor  $g_i$  as in Equation (4) and allowing the available-volume fractions to be arbitrary functions of the particle densities and temperature. The medium dependence of the effective degeneracy factors is interpreted as a change in the effective number of degrees of freedom. A decrease in  $g_i^{(\text{eff})}$  has the effect of a repulsive interaction between the particles, whereas an increase can be seen as the action of an attractive interaction, c.f., the softening of the nuclear EoS when hyperons are included, see, e.g., [26,27]. This freedom leaves the room to modify the properties of an EoS in a favored way.

In the present application of the modified EV mechanism, the available-volume fraction is defined to be identical for all particles  $i$  as

$$\Phi_i = 1 + sg_1(T)\theta(x) \exp\left(-\frac{1}{2x^2}\right) \quad (30)$$

depending on the temperature  $T$  and an auxiliary quantity

$$x = v \left( \sum_j B_j n_j^{(v)} - g_8(T) n_{\text{cut}} \right) \quad (31)$$

depending on  $T$  and the quasi-particle vector densities  $n_i^{(v)}$  with parameters  $s$ ,  $v$ , and a cutoff density of  $n_{\text{cut}}$ . The  $\theta$  function in Equation (30) guarantees that  $\Phi_i = 1$  for  $x \leq 0$  and the EV mechanism has no effect on the EoS. The functions  $g_1$  in Equation (30) and  $g_8$  in Equation (31) are defined as

$$g_t(T) = \theta(T_0 - T) \exp\left[-\frac{t}{2} \left(\frac{T}{T_0 - T}\right)^2\right] \quad (32)$$

with parameters  $t$  and  $T_0$ . In the limit  $T \rightarrow 0$ , the function  $g_t$  approaches one and it decreases with increasing temperature. Furthermore, the derivatives  $\partial\Phi_i/\partial T$  approach zero for  $T \rightarrow 0$ , as required for the thermodynamic consistency, because of the choice of the function  $g_t(T)$ . For  $T \rightarrow T_0$ , the function  $g_t$  vanishes very smoothly and there are no effects at higher temperatures because  $\Phi_i = 1$ . In order to reproduce the correct high-temperature limit, given by a Stefan–Boltzmann-type behavior, a modification of the available-volume fractions for temperatures well above  $T_0$  is required. This is left to future extensions of the model. According to Equation (31), the quantity  $x$  is only positive for baryon densities larger than  $g_8 n_{\text{cut}}$ , a quantity that decreases with increasing temperature. There are no artificial singularities due to the presence of the  $\theta$  functions in Equations (30) and (32) because all derivatives of the exponential functions are zero when the arguments of the  $\theta$  functions vanish. The actual values of the parameters for the modified EV mechanism used in the present study are  $s = 3$ ,  $v = 2 \text{ fm}^3$ ,  $T_0 = 270 \text{ MeV}$ , and  $n_{\text{cut}} = n_{\text{sat}}$  of the DD2 parametrization.

### 3. Results

In order to illustrate the characteristic effects of the modified EV mechanism on the EoS, we limit the presentation to the case of symmetric matter, i.e.,  $Y_q = 0.5$ . The pressure  $p$  and baryon chemical potential  $\mu_B$  are calculated as a function of the baryon density  $n_B$ . Due to the increase in the available-volume fractions  $\Phi_i$  or the effective degeneracy factors  $g_i^{(\text{eff})}$ , a considerable softening of the EoS is observed in a certain range of densities. Below the critical temperature  $T_{\text{crit}}$ , the pressure is not a monotonous function of the baryon chemical potential for an isotherm. A Maxwell construction is used to determine the two densities of the coexisting phases where  $p$  and  $\mu_B$  are identical. The pressure  $p$  as a function of the baryon density  $n_B$  is depicted in Figure 1 for selected temperatures. Note that an integral part of the underlying RMF model is a detailed description of the liquid–gas PT in nuclear matter and the formation and dissociation of nuclear clusters in compact-star matter. For details, see, e.g., [28].

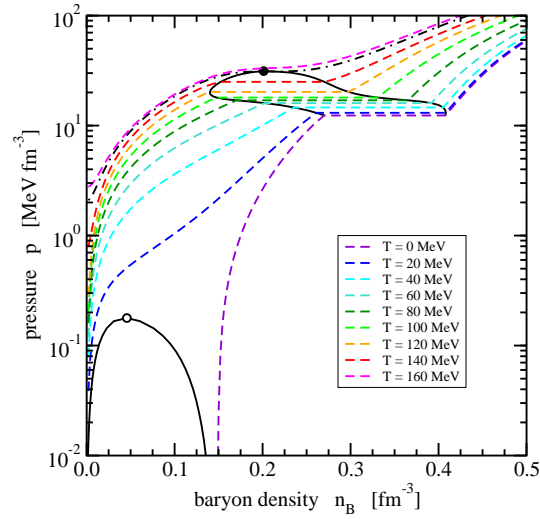


**Figure 1.** Isotherms in isospin-symmetric strongly interacting matter in the pressure–baryon density diagram at temperatures from 0 to 160 MeV in steps of 20 MeV (dashed colored lines) and at the critical temperature  $T_{\text{crit}}$  of the pseudo hadron–quark phase transition (black dot-dashed line). The binodals and critical points are denoted by full black lines and a full (open) circle of the pseudo hadron–quark (liquid–gas) phase transition, respectively.

In the coexistence region of the pseudo hadron–quark PT between the low and high density phases, the pressure is constant as typical for a first-order PT. The area of coexistence is enclosed by the binodal, and, above the critical temperature  $T_{\text{crit}} \approx 155.5$  MeV, there is no PT anymore. The peculiar shape of the binodal is a result of the specific form (30) of the available-volume fractions. It can be adjusted with appropriate changes in the functional form and parameters.

The binodals of the liquid–gas and pseudo hadron–quark PT in the temperature–baryon density plane are shown in panel (a) of Figure 2. At vanishing temperatures, the coexistence region of the pseudo hadron–quark PT covers a density range from  $0.270$  to  $0.408 \text{ fm}^{-3}$ , well above the nuclear saturation density  $n_{\text{sat}}$ . At higher temperatures, it moves to lower densities with an almost constant extension in baryon density except for temperatures close to  $T_{\text{crit}}$ . Here, the critical density is found as  $0.201 \text{ fm}^{-3}$ , still above  $n_{\text{sat}}$ . The dashed line in panel (a) marks the boundary between regions without (lower left) and with (upper right) effects of the modified EV mechanism in the present parametrization. It corresponds to the condition  $x = 0$ . There is another region in the phase diagram without modified EV effects at temperatures above  $T_0$ , outside the figure.

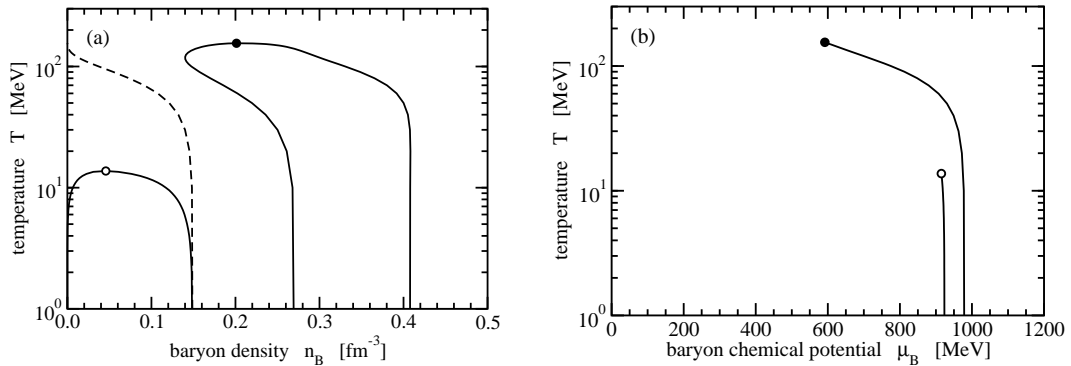


**Figure 2.** Binodals (full lines) and critical points (full and open circles) of isospin-symmetric strongly interacting matter in (a) the temperature–baryon density diagram and (b) the temperature–baryon chemical potential diagram. The dashed line in panel (a) separates the region without effects of the modified excluded-volume mechanism (lower left) from the region with effects (upper right). Results for the liquid–gas phase transition are shown at subsaturation densities.



Panel (b) of Figure 2 depicts the lines of the first-order PT in the temperature–baryon chemical potential diagram ending in critical points. With increasing temperature, the baryon chemical potential at the pseudo hadron–quark PT reduces from 979.1 to 591.8 MeV at the critical point. By crossing the transition line, an abrupt change in the density occurs that becomes continuous at the critical point.

#### 4. Conclusions

The extension of the modified EV approach to a density- and temperature-dependent parametrization of the available-volume fractions as introduced in this work was successful in achieving the main goal of this study: As a generic structure of the QCD phase diagram, a first-order pseudo hadron–quark phase transition at low temperatures and a crossover for low baryon densities could be modeled that also includes a critical endpoint at  $T_{\text{crit}} = 155.5$  MeV and  $\mu_{B,\text{crit}} = 591.8$  MeV. Other patterns of the QCD phase diagram that have been theoretically motivated could also be modeled within the present approach. Further extensions of the model are straightforward. They include the extension to a larger number of components of the hadron resonance gas in the underlying RMF model and an isospin dependence of the EV model. It would be worthwhile to study further thermodynamic quantities such as the speed of sound, heat capacities, or the susceptibilities in such an enlarged model. It would also be interesting to elaborate on a parametrization that would result in a second endpoint at low temperatures, as suggested by Hatsuda et al. [14]. The so-generalized parametrization of the QCD EoS can be used in Bayesian analysis studies for astrophysical applications pertaining to compact stars [29,30], their mergers, and core-collapse supernova explosions, as well as heavy-ion collisions analogous to those studied in [31].

**Acknowledgments:** This work was supported by the Russian Science Foundation under contract number 17-12-01427. S.T. was supported in part by the DFG through grant No. SFB1245.

**Author Contributions:** D.B. and S.T. conceived and designed the concept of this work. S.T. worked out the theoretical framework, performed the numerical calculations and wrote the main body of the paper. D.B. contributed abstract, discussion, conclusions and references.

**Conflicts of Interest:** The authors declare no conflict of interest.

#### Abbreviations

The following abbreviations are used in this manuscript:

CCSN	core-collapse supernova
EoS	equation of state
EV	excluded-volume
HIC	heavy-ion collision
NS	neutron star
PT	phase transition
QCD	quantum chromodynamics
RMF	relativistic mean-field

#### References

1. Alford, M.G.; Han, S.; Prakash, M. Generic conditions for stable hybrid stars. *Phys. Rev.* **2013**, *D88*, 083013, [arXiv:astro-ph.SR/1302.4732].
2. Benic, S.; Blaschke, D.; Alvarez-Castillo, D.E.; Fischer, T.; Typel, S. A new quark-hadron hybrid equation of state for astrophysics - I. High-mass twin compact stars. *Astron. Astrophys.* **2015**, *577*, A40, [arXiv:astro-ph.HE/1411.2856].
3. Alvarez-Castillo, D.E.; Blaschke, D.B. High-mass twin stars with a multipolytrope equation of state. *Phys. Rev.* **2017**, *C96*, 045809, [arXiv:nucl-th/1703.02681].



4. Sagert, I.; Fischer, T.; Hempel, M.; Pagliara, G.; Schaffner-Bielich, J.; Mezzacappa, A.; Thielemann, F.K.; Liebendörfer, M. Signals of the QCD phase transition in core-collapse supernovae. *Phys. Rev. Lett.* **2009**, *102*, 081101, [[arXiv:astro-ph/0809.4225](#)].
5. Fischer, T.; Whitehouse, S.C.; Mezzacappa, A.; Thielemann, F.K.; Liebendörfer, M. The neutrino signal from protoneutron star accretion and black hole formation. *Astron. Astrophys.* **2009**, *499*, 1, [[arXiv:astro-ph/0809.5129](#)].
6. Fischer, T.; Sagert, I.; Pagliara, G.; Hempel, M.; Schaffner-Bielich, J.; Rauscher, T.; Thielemann, F.K.; Käppeli, R.; Martínez-Pinedo, G.; Liebendörfer, M. Core-collapse supernova explosions triggered by a quark-hadron phase transition during the early post-bounce phase. *Astrophys. J. Suppl.* **2011**, *194*, 39, [[arXiv:astro-ph.HE/1011.3409](#)].
7. Fischer, T.; Bastian, N.U.; Blaschke, D.; Cerniak, M.; Hempel, M.; Klähn, T.; Martínez-Pinedo, G.; Newton, W.G.; Röpke, G.; Typel, S. The state of matter in simulations of core-collapse supernovae – Reflections and recent developments. 2017, [[arXiv:astro-ph.HE/1711.07411](#)].
8. Blaschke, D.B.; Sandin, F.; Skokov, V.V.; Typel, S. Accessibility of Color Superconducting Quark Matter Phases in Heavy-ion Collisions. *Acta Phys. Polon. Supp.* **2010**, *3*, 741–746, [[arXiv:hep-ph/1004.4375](#)].
9. Bazavov, A.; others. Equation of state in (2+1)-flavor QCD. *Phys. Rev.* **2014**, *D90*, 094503, [[arXiv:hep-lat/1407.6387](#)].
10. Borsanyi, S.; Fodor, Z.; Hoelbling, C.; Katz, S.D.; Krieg, S.; Szabo, K.K. Full result for the QCD equation of state with 2+1 flavors. *Phys. Lett.* **2014**, *B730*, 99–104, [[arXiv:hep-lat/1309.5258](#)].
11. Bratovic, N.M.; Hatsuda, T.; Weise, W. Role of Vector Interaction and Axial Anomaly in the PNJL Modeling of the QCD Phase Diagram. *Phys. Lett.* **2013**, *B719*, 131–135, [[arXiv:hep-ph/1204.3788](#)].
12. Baym, G.; Hatsuda, T.; Kojo, T.; Powell, P.D.; Song, Y.; Takatsuka, T. From hadrons to quarks in neutron stars 2017. [[arXiv:astro-ph.HE/1707.04966](#)].
13. Abuki, H.; Baym, G.; Hatsuda, T.; Yamamoto, N. The NJL model of dense three-flavor matter with axial anomaly: the low temperature critical point and BEC-BCS diquark crossover. *Phys. Rev.* **2010**, *D81*, 125010, [[arXiv:hep-ph/1003.0408](#)].
14. Hatsuda, T.; Tachibana, M.; Yamamoto, N.; Baym, G. New critical point induced by the axial anomaly in dense QCD. *Phys. Rev. Lett.* **2006**, *97*, 122001, [[arXiv:hep-ph/0605018](#)].
15. Klähn, T.; Fischer, T. Vector interaction enhanced bag model for astrophysical applications. *Astrophys. J.* **2015**, *810*, 134, [[arXiv:nucl-th/1503.07442](#)].
16. Dexheimer, V.A.; Schramm, S. A Novel Approach to Model Hybrid Stars. *Phys. Rev.* **2010**, *C81*, 045201, [[arXiv:astro-ph.SR/0901.1748](#)].
17. Mukherjee, A.; Steinheimer, J.; Schramm, S. Higher-order baryon number susceptibilities: interplay between the chiral and the nuclear liquid-gas transitions. *Phys. Rev.* **2017**, *C96*, 025205, [[arXiv:nucl-th/1611.10144](#)].
18. Vovchenko, V.; Pasztor, A.; Fodor, Z.; Katz, S.D.; Stoecker, H. Repulsive baryonic interactions and lattice QCD observables at imaginary chemical potential. *Phys. Lett.* **2017**, *B775*, 71–78, [[arXiv:hep-ph/1708.02852](#)].
19. Typel, S. Variations on the excluded-volume mechanism. *Eur. Phys. J.* **2016**, *A52*, 16.
20. Oertel, M.; Hempel, M.; Klähn, T.; Typel, S. Equations of state for supernovae and compact stars. *Rev. Mod. Phys.* **2017**, *89*, 015007, [[arXiv:astro-ph.HE/1610.03361](#)].
21. Rischke, D.H.; Gorenstein, M.I.; Stoecker, H.; Greiner, W. Excluded volume effect for the nuclear matter equation of state. *Z. Phys.* **1991**, *C51*, 485–490.
22. Satarov, L.M.; Dmitriev, M.N.; Mishustin, I.N. Equation of state of hadron resonance gas and the phase diagram of strongly interacting matter. *Phys. Atom. Nucl.* **2009**, *72*, 1390–1415, [[arXiv:hep-ph/0901.1430](#)].
23. Typel, S.; Röpke, G.; Klähn, T.; Blaschke, D.; Wolter, H.H. Composition and thermodynamics of nuclear matter with light clusters. *Phys. Rev.* **2010**, *C81*, 015803, [[arXiv:nucl-th/0908.2344](#)].
24. Vovchenko, V.; Gorenstein, M.I.; Stoecker, H. van der Waals Interactions in Hadron Resonance Gas: From Nuclear Matter to Lattice QCD. *Phys. Rev. Lett.* **2017**, *118*, 182301, [[arXiv:hep-ph/1609.03975](#)].
25. Hempel, M.; Schaffner-Bielich, J. Statistical Model for a Complete Supernova Equation of State. *Nucl. Phys.* **2010**, *A837*, 210–254, [[arXiv:nucl-th/0911.4073](#)].
26. Chatterjee, D.; Vidaña, I. Do hyperons exist in the interior of neutron stars? *Eur. Phys. J.* **2016**, *A52*, 29, [[arXiv:nucl-th/1510.06306](#)].

27. Schaffner-Bielich, J. Hypernuclear Physics for Neutron Stars. *Nucl. Phys.* **2008**, *A804*, 309–321, [[arXiv:astro-ph/0801.3791](#)].
28. Typel, S.; Wolter, H.H.; Röpke, G.; Blaschke, D. Effects of the liquid-gas phase transition and cluster formation on the symmetry energy. *Eur. Phys. J.* **2014**, *A50*, 17, [[arXiv:nucl-th/1309.6934](#)].
29. Steiner, A.W.; Lattimer, J.M.; Brown, E.F. The Equation of State from Observed Masses and Radii of Neutron Stars. *Astrophys. J.* **2010**, *722*, 33–54, [[arXiv:astro-ph.HE/1005.0811](#)].
30. Alvarez-Castillo, D.; Ayriyan, A.; Benic, S.; Blaschke, D.; Grigorian, H.; Typel, S. New class of hybrid EoS and Bayesian M-R data analysis. *Eur. Phys. J.* **2016**, *A52*, 69, [[arXiv:nucl-th/1603.03457](#)].
31. Pratt, S.; Sangaline, E.; Sorensen, P.; Wang, H. Constraining the Eq. of State of Super-Hadronic Matter from Heavy-Ion Collisions. *Phys. Rev. Lett.* **2015**, *114*, 202301, [[arXiv:nucl-th/1501.04042](#)].



© 2018 by the authors. Licensee MDPI, Basel, Switzerland. This article is an open access article distributed under the terms and conditions of the Creative Commons Attribution (CC BY) license (<http://creativecommons.org/licenses/by/4.0/>).